Macromolecules

ARTICLE

pubs.acs.org/Macromolecules

Influence of Zwitterions on Thermomechanical Properties and Morphology of Acrylic Copolymers: Implications for Electroactive Applications

Tianyu Wu,[†] Frederick L. Beyer,[*,‡] Rebecca H. Brown,[†] Robert B. Moore,[†] and Timothy E. Long[*,†]

[†]Department of Chemistry, Macromolecules and Interfaces Institute, Virginia Tech, Blacksburg, Virginia 24061-0212, United States

[‡]Army Research Laboratory, Aberdeen Proving Ground, Maryland 21005-5069, United States

Supporting Information

ABSTRACT: *n*-Butyl acrylate-based zwitterionomers and ionomers containing 3-[[2-(methacryloyloxy)ethyl](dimethyl)-ammonio]-1-propanesulfonate (SBMA) and 2-[butyl(dimethyl)-amino]ethyl methacrylate methanesulfonate (BDMAEMA MS), respectively, were synthesized using conventional free radical polymerization. Size-exclusion chromatography confirmed the molecular weights of the copolymers exceeded the critical molecular weight between entanglements (M_e) for poly(*n*-butyl acrylate). Differential scanning calorimetry (DSC), small-angle X-ray scattering (SAXS), and atomic force microscopy (AFM) revealed that zwitterionomers promoted more well-defined microphase separation than cationic analogues. Dynamic mechanical analyses (DMA) of the copolymers showed a rubbery plateau region due to physical cross-links between charges for zwitterionomers only. Since SBMA and BDMAEMA MS have very similar chemical structures, we attributed improved microphase separation and superior elastomeric performance of the zwitterionomers to stronger association between covalently tethered charged pairs.

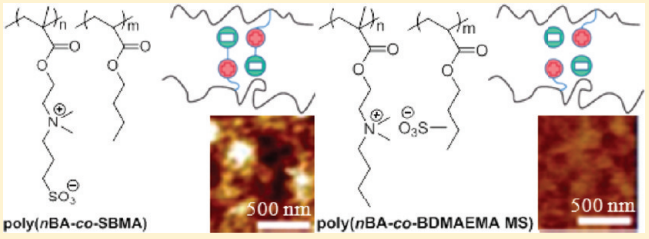

INTRODUCTION

Charge-containing polymers have attracted considerable scientific attention over the past 20 years.[1−3] They offer tremendous impact in emerging technologies ranging from energy[4] and water purification[5] to biotechnology.[6] A unique combination of physical properties of ionomeric membranes is the ionic conductivity of low molar mass electrolytes and viscoelastic response of polymers in the solid state. For example, our research group demonstrated the fabrication of ionic polymer transducers from branched sulfonated polysulfones.[7] The mechanical strength of the membranes drastically decreased upon introduction of ionic liquids to impart ionic conductivity. For electroactive applications, it is desirable for ionomeric membranes to maintain mechanical strength despite the presence of plasticizing conductive electrolytes. Recently, we investigated the versatility of zwitterion-containing acrylic copolymers to absorb ionic liquids,[8] and zwitterionomers maintained mechanical strengths upon swelling with 10 wt % ionic liquid.

Zwitterions are charged molecules that contain equal numbers of covalently bound cations and anions. The unique presence of opposite charges bridged through alkylene spacers offers zwitterions extremely high polarity. Typical dipole moments of sulfobetaine-type zwitterions are reported as $\mu \sim 18.7-27.6$ D based on calculations,[9] whereas water is only 1.9 D. Therefore, strong electrostatic interactions are ubiquitous among zwitterions. Galin and co-workers studied extensively the solid-state properties of ethyl acrylate and *n*-butyl acrylate (*n*BA)-based sulfobetaine-containing copolymers.[10,11] They found that the incorporation of zwitterionic functionalities afforded elastomeric properties, which were typical for ionomers with low-T_g polymeric matrices.[10,12−14] Detailed morphological studies revealed that zwitterionomers adopted morphologies that were in agreement with the Eisenberg−Hird−Moore multiplet-cluster model.[15] In addition, Laschewsky et al. have shown that polymeric betaines have remarkable miscibility with various inorganic and metal salts approaching stoichiometric quantities.[16] Galin and co-workers have also demonstrated that these salt−polyzwitterion mixtures formed amorphous blends due to strong ion-dipole interactions that precluded salt segregation or crystallization within the zwitterionic matrix.[17,18] This unique ability to dissolve large amounts of salts has sparked interest in polyzwitterions as polymeric host matrices for many polar guest molecules.

While zwitterionic polymers have exhibited many unique physical properties, their difference from cationic or anionic polymers is not well-established. Lee and co-workers investigated the difference in solution properties between poly(sulfobetaine)s homopolymers and their corresponding cationic polymers.[19−21] However, the cationic models contained iodide anions rather than monovalent sulfonate anions, which are present in sulfobetaines. Our work describes 2-(*n*-butyldimethylamino)ethyl

Received: May 28, 2011
Revised: September 4, 2011
Published: September 30, 2011

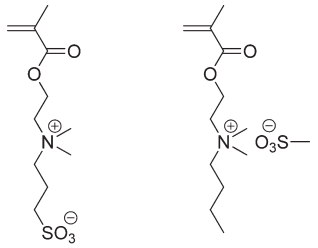

Figure 1. SBMA and BDMAEMA MS monomers.

2-methacrylate methanesulfonate (BDMAEMA MS), as shown in Figure 1, along with 3-[[2-(methacryloyloxy)ethyl](dimethyl)-ammonio]-1-propanesulfonate (SBMA), a zwitterionic monomer. Copolymerization of both charge-containing monomers with *n*BA elucidates the influence of tethered counterions on the solid-state properties and morphology of zwitterionomers. Thermogravimetric analysis (TGA), differential scanning calorimetry (DSC), and dynamic mechanical analysis (DMA) probed thermal stability, glass transition temperatures, and thermomechanical behavior of the copolymers, respectively. Small-angle X-ray scattering (SAXS) and atomic force microscopy (AFM) imaging results showed the morphological differences between the two copolymer series. A correlation between the elastomeric performance of the copolymers and their morphologies revealed the impact of zwitterionic interactions and ammonium ionic interactions with mobile counteranions. Fundamental understanding of structure−morphology relationships will guide the design of future charge-containing polymers for advanced transducer applications.

EXPERIMENTAL SECTION

Materials. Zwitterionic monomer, 3-[[2-(methacryloyloxy)ethyl]-(dimethyl)ammonio]-1-propanesulfonate (SBMA), was generously provided by Raschig GmbH. *n*-Butyl acrylate (*n*BA, Alfa Aesar, 98+%) and 2-(dimethylamino)ethyl methacrylate (DMAEMA, Aldrich, 98%) were deinhibited using neutral alumina columns. *n*BA was further distilled under reduced pressure from calcium hydride. Azobis(isobutyronitrile) (AIBN, Aldrich, 98%) was recrystallized from methanol. Dimethyl sulfoxide (DMSO, Alfa Aesar, 99.9+%), hydroquinone (Alfa Aesar, 99%), 1-bromobutane (Aldrich, 98%), silver methanesulfonate (AgMS, Aldrich), and diethyl ether (Mallinckrodt, anhydrous) were used as received. Ultrapure water having a resistivity of 18.2 MΩ · cm was obtained using a Millipore Direct-Q5 purification system.

Synthesis of 2-(*N*-Butyl-*N*,*N*-dimethylamino)ethyl Methacrylate Methanesulfonate (BDMAEMA MS). DMAEMA (30.0 g, 0.191 mol), 1-bromobutane (52.3 g, 0.388 mol), methylene chloride (40 mL, 35 vol %), and hydroquinone (6.0 g) were added to a 250 mL, round-bottomed flask with a magnetic stir bar. The reaction mixture was sparged with N_2 for 15 min and placed into an oil bath at 50 °C for 72 h. The product, 2-(*N*-butyl-*N*,*N*-dimethylamino)ethyl methacrylate bromide (BDMAEMA Br), was precipitated into and washed with dry ether, recrystallized from acetone, and dried under reduced pressure (0.5 mmHg) at room temperature. A yield of 70% was obtained. Anion exchange of BDMAEMA Br was then conducted at room temperature. AgMS (1.00 g, 4.92 mmol) and BDMAEMA Br (1.45 g, 4.93 mmol) were dissolved in 15 and 5 mL of Milli-Q water, respectively, in 20 mL scintillation vials. After full dissolution, the AgMS solution was transferred to a 120 mL amber container, and the BDMAEMA Br solution was subsequently added in the absence of light. Both vials were thoroughly rinsed with Milli-Q water after solution transfer. The reaction was allowed to equilibrate in the dark overnight, although the precipitation of AgBr was instantaneous. The BDMAEMA MS solution was finally filtered through a fine fritted funnel and lyophilized dry. A yield of 97% was obtained. ^{1}H NMR (400 MHz, D_2O, δ): 0.95 (t, J = 8.0 Hz, 3H), 1.38 (m, 2H), 1.78 (m, 2H), 1.94 (s, 3H), 2.80 (s, 3H), 3.17 (s, 6H), 3.40 (m, 2H), 3.77 (m, 2H), 4.63 (m, 2H), 5.79 (s, 1H), 6.16 (s, 1H).

Synthesis of Poly(*n*BA-*co*-SBMA) and Poly(*n*BA-*co*-BDMAEMA MS). A typical copolymerization of poly(*n*BA-*co*-SBMA) containing 10 mol % SBMA is described as follows: *n*BA (5.00 g, 39.1 mmol), SBMA (1.21 g, 4.33 mmol), and AIBN (31.1 mg) were charged to a 150 mL round-bottomed flask with a magnetic stir bar. DMSO (51.1 mL, 90 wt %) was added to dissolve the monomers. The reaction mixture was sparged with N_2 for 15 min and placed into an oil bath at 65 °C for 24 h. The polymer was precipitated into water and allowed to equilibrate in ultrapure water for a week. A yield of 90% was obtained. The final product was monomer-free, as confirmed using ^{1}H NMR spectroscopy, and any residual DMSO was removed with reduced pressure at 65 °C for 3 days.

The syntheses of poly(*n*BA-*co*-BDMAEMA MS) were conducted under similar conditions with 10 wt % monomer in the reaction mixture and 0.5 wt % AIBN based on total monomer. However, the cationic analogues were first isolated with vacuum stripping of DMSO due to very different solubility. The products were subsequently dissolved in methanol and diluted with ultrapure water. The product solutions remained homogeneous upon H_2O addition and upon removal of methanol. Purification of the copolymers was performed using exhaustive dialysis, and ^{1}H NMR spectra also confirmed the absence of residue monomer. Typical yields of 85% were achieved.

Instrumentation. ^{1}H NMR spectra were obtained on a Varian Unity 400 MHz spectrometer in D_2O, $CDCl_3$, and CD_3OD. Size exclusion chromatography (SEC) determined the molecular weights of the copolymers at 50 °C in DMF with 0.01 M LiBr at 1 mL min^{-1} flow rate. The DMF SEC system was equipped with a Waters 717plus autosampler, a Waters 1525 HPLC pump, two Waters Styragel HR5E (DMF) columns, and a Wyatt miniDAWN multiangle laser light scattering (MALLS) detector. Absolute molecular weights, as well as the specific refractive index increments (dn/dc) for all the samples, were determined using the Wyatt Astra V software package.

Thermogravimetric analysis (TGA) of the samples employed a TA Q500 from 25 to 700 °C at a heating rate of 10 °C min^{-1} under a N_2 atmosphere. Differential scanning calorimetry (DSC) measurements were performed on a TA Q100 instrument at a heating and cooling rate of 10 °C/min from −90 °C. The first heat scans were concluded at 120 °C, and traces of the second heats are reported. Dynamic mechanical analysis (DMA) was performed on a TA Q800 analyzer in tension mode, at 1 Hz frequency, 15 μm amplitude, and 3 °C/min heating rate from −90 °C. The copolymer membranes were cast from 0.1 g mL^{-1} chloroform solutions into Teflon molds to achieve film thicknesses of ∼0.30 mm. The films were dried at 25 °C overnight and subsequently heated at 65 °C for 72 h under vacuum prior to physical characterizations.

A Veeco MultiMode scanning probe microscope was used with Veeco MPP-21100-10 tips with spring constants of 3 N/m for tapping-mode AFM imaging. Samples were imaged at a set-point to free-air amplitude ratio of 0.6 and at magnifications of 600 nm × 600 nm.

Small-angle X-ray scattering data were collected with a customized, pinhole collimated 3 m camera. X-rays were generated with a Rigaku Ultrax18 rotating Cu anode generator operated at 45 kV and 100 mA and then filtered with Ni foil to select the Cu Kα doublet (λ = 1.542 Å). Two-dimensional data sets were collected using a Molecular Metrology multiwire area detector at both 50 and 150 cm from the detector. Raw data were corrected for absorption and background noise and subsequently azimuthally averaged. The corrected data were placed on an absolute scale using a secondary standard, type 2 glassy carbon, and the data at both camera lengths were subsequently merged into

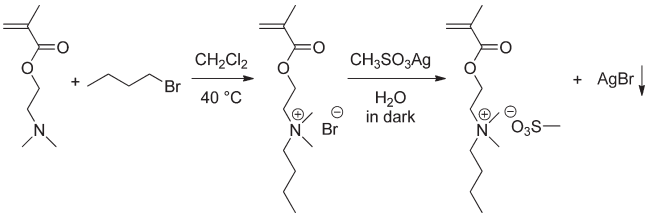

Figure 2. Synthesis of BDMAEMA Br in the presence of free radical inhibitor (hydroquinone) and subsequent anion exchange to BDMAEMA MS.

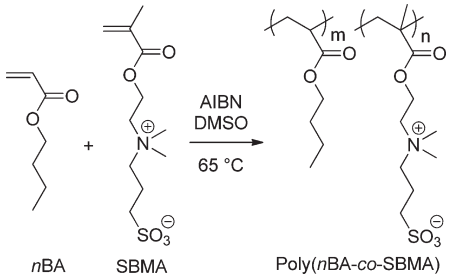

Figure 3. Synthesis of poly(*n*BA-*co*-SBMA) using conventional free radical polymerization.

one continuous data set for each sample. All data reduction and analysis were performed using Igor Pro v6.12A from Wavemetrics, Inc., using a suite of procedures developed at the Argonne National Laboratory.[22]

RESULTS AND DISCUSSION

Synthesis and Characterization of BDMAEMA MS. The synthesis of BDMAEMA MS is illustrated in Figure 2. The structure of this novel monomer was confirmed using ^{1}H NMR spectroscopy (Figure S1), ^{13}C NMR spectroscopy (Figure S2), and elemental analysis (Table S1). A melting point of 160 °C was observed in the first heat of the DSC. There are earlier reports of quaternized DMAEMAs bearing a butyl group and various halide anions, such as Cl, Br, and I, or PF_6 anion.[23−26] In our study, we designed BDMAEMA MS to serve as the appropriate cationic analogue to SBMA as shown in Figure 1. Both structures contain quaternary ammonium cations and monovalent sulfonate anions. The butyl group in BDMAEMA MS was chosen to match the spacer length between charges in SBMA.

Synthesis and Structural Characterization of Poly(*n*BA-*co*-SBMA) and Poly(*n*BA-*co*-BDMAEMA MS). Zwitterionic copolymers containing 3, 6, and 9 mol % SBMA were synthesized using conventional free radical copolymerization in DMSO. A typical synthesis of poly(*n*BA-*co*-SBMA) is depicted in Figure 3. The reactions reached high conversions in 24 h. ^{1}H NMR spectra confirmed that the products were monomer-free. The amount of SBMA in the copolymer was determined using ^{1}H NMR spectroscopy. However, any compositional drift due to high conversion was not determined.

The cationic analogues containing 7, 10, 15, and 22 mol % BDMAEMA MS were synthesized under similar conditions to those for zwitterionomers. However, the product isolation step was quite different due to very different solubility between the zwitterionomers and their cationic analogues. Nevertheless, the absence of the monomers in the final products was also confirmed

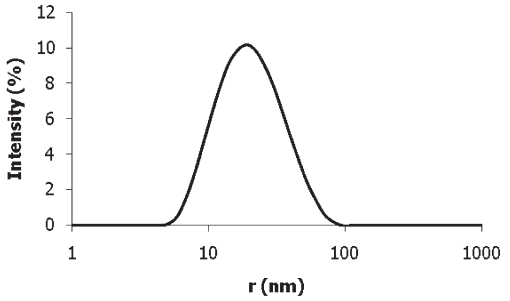

Figure 4. DLS intensity vs radius plot of poly(nBA$_{91}$-*co*-SBMA$_9$) in DMF with 0.01 M LiBr.

using ^{1}H NMR spectra. The copolymer compositions were confirmed using ^{1}H NMR spectroscopy.

The molecular weight determination of charge-containing polymers using size exclusion chromatography often presents a challenge due to ionic association of the polymers in solution. We demonstrated the use of dynamic light scattering in the screening of suitable SEC solvents for water-soluble ionenes.[27] In this current study, we adopted the same methodology and determined that DMF with 0.01 M LiBr was a suitable SEC eluent for both poly(*n*BA-*co*-SBMA) and poly(*n*BA-*co*-BDMAEMA MS). Figure 4 is a representative DLS trace of poly(nBA$_{91}$-*co*-SBMA$_9$) in DMF with 0.01 M LiBr. The single peak with an average diameter of 23 nm suggested the absence of aggregation in the SEC solvent system.

SEC reproducibility tests confirmed that the SEC condition was suitable for both copolymer systems, except for the cationic analogue containing 22 mol % BDMAEMA MS. We attributed the irreproducibility of this sample to the interaction between the polymer and the column at high BDMAEMA MS compositions. Table 1 lists the absolute molecular weights of the copolymers as well as their specific refractive index increments. Since the average molecular weight between chain entanglements (M_e) for poly(*n*BA) is 28K,[28] our samples were of sufficient molecular weight for reliable thermomechanical property characterization. Molecular weight distribution values above 2.0 were typical of *n*BA-containing polymers synthesized with free radical processes.[29,30]

Thermal Characterization of Zwitterionomers and Cationic Analogues. The thermal stability of the copolymers was determined using thermogravimetric analysis. Figure 5 shows representative TGA traces of copolymers containing 9 mol % SBMA and 10 mol % BDMAEMA MS. The 5% mass loss temperatures of poly(*n*BA-*co*-SBMA) were ∼300 °C, while poly(*n*BA-*co*-BDMAEMA MS) was similar. Burch and Manring showed that the thermal degradation of quaternary ammonium-containing polymers follow the Hofmann elimination mechanism.[31] Since the MS anion in BDMAEMA MS has similar basicity to the sulfonate group in SBMA, it was expected that the copolymer containing 9 mol % SBMA would have similar 5% weight loss temperature to its cationic analogue. TGA results also suggested that enhanced mobility of MS anions in BDMAEMA MS did not facilitate abstraction of β-H of the quaternary ammonium to initiate the degradation process.

Differential scanning calorimetry results exhibited one glass transition temperature for all copolymers, and T_g values are summarized in Table 2. For the zwitterionomers, the glass transition temperatures increased only slightly from −47 °C for poly(*n*BA) to −40 °C for copolymers containing 9 mol % SBMA. Considering that the glass transition temperature of poly(SBMA) was

Table 1. Size Exclusion Chromatographic Analysis

copolymer composition	dn/dc (mL/g)	M_n (kg/mol)	M_w (kg/mol)	M_w/M_n
poly(nBA$_{97}$-*co*-SBMA$_3$)	0.045	87.1	461	5.28
poly(nBA$_{94}$-*co*-SBMA$_6$)	0.049	183	472	2.57
poly(nBA$_{91}$-*co*-SBMA$_9$)	0.050	162	404	2.49
poly[nBA$_{93}$-*co*-BDMAEMA MS$_7$]	0.047	115	294	2.55
poly[nBA$_{90}$-*co*-BDMAEMA MS$_{10}$]	0.051	88.7	228	2.56
poly[nBA$_{85}$-*co*-BDMAEMA MS$_{15}$]	0.042	246	252	1.03

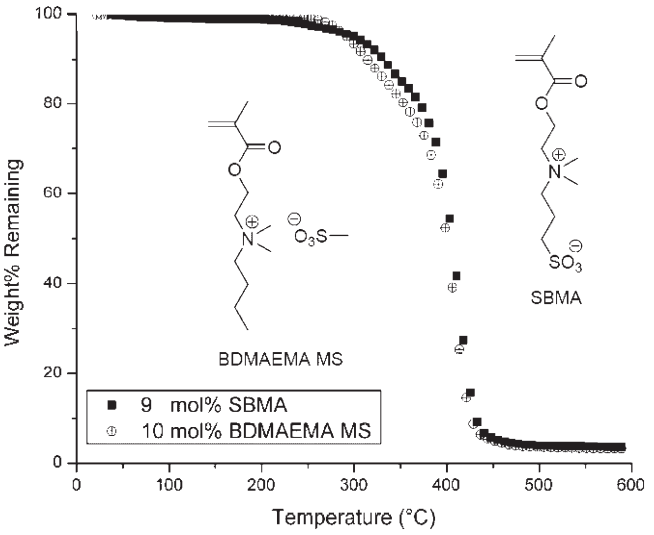

Figure 5. TGA of poly(*n*BA-*co*-SBMA) and poly(*n*BA-*co*-DBMAEMA MS) containing ~10 mol % of charged units.

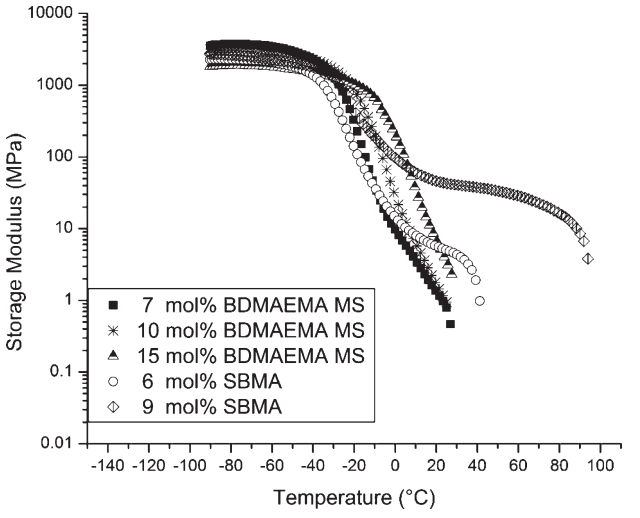

Figure 6. Storage modulus vs temperature profiles for poly(*n*BA-*co*-SBMA) and poly(*n*BA-*co*-BDMAEMA MS) containing varying amounts of charged units.

Table 2. Glass Transition Temperatures of Zwitterionomers and Their Cationic Analogues

copolymer composition	T_g (°C)
poly(nBA)	−47
poly(nBA$_{97}$-*co*-SBMA$_3$)	−44
poly(nBA$_{94}$-*co*-SBMA$_6$)	−42
poly(nBA$_{91}$-*co*-SBMA$_9$)	−40
poly(SBMA)	203
poly[nBA$_{93}$-*co*-(BDMAEMA MS)$_7$]	−35
poly[nBA$_{90}$-*co*-(BDMAEMA MS)$_{10}$]	−26
poly[nBA$_{85}$-*co*-(BDMAEMA MS)$_{15}$]	−5
poly[nBA$_{78}$-*co*-(BDMAEMA MS)$_{22}$]	19
poly(BDMAEMA MS)	83

203 °C, the observed T_g corresponded to the poly(*n*BA)-rich phase. This was an indication that the zwitterionomers presented biphasic morphologies, and the lack of a second T_g was likely due to low SBMA contents in the copolymers in agreement with a previous report on similar copolymers.[14] In comparison, the T_g of the cationic analogue containing 7 mol % BDMAEMA MS was −35 °C, higher than the 9 mol % zwitterionomer. Further increasing the charged contents in the cationic analogue to 22 mol % resulted in a glass transition temperature of 19 °C for the copolymer. The different trends of T_g increase with increasing charge contents suggested that the zwitterionomers provided a more well-defined microphase-separated morphology than their cationic analogues.

Mechanical Characterization of Zwitterionomers and Their Cationic Analogues. Dynamic mechanical analysis provided the thermomechanical behavior of the copolymers. Figure 6 shows the DMA traces of the zwitterionomers and their cationic analogues. In agreement with the DSC results, the glass transitions for both 6 and 9 mol % zwitterionomers appeared at approximately the same temperature, while the cationic analogues increased steadily with increasing charge contents in the copolymers. Because of the frequency dependence of polymer chain segmental motion, the glass transition temperatures of the samples measured using DMA were higher than values measured using DSC. More importantly, rubbery plateaus were observed only for zwitterionomers, in sharp contrast for cationic analogues. Gauthier and Eisenberg were among the first to systematically study similar rubbery plateaus observed in poly(styrene)-based ionomers.[32] They attributed the presence of rubbery plateaus to the physical cross-linking induced by ionic associations between metal cations and carboxylate anions. Here, we attributed rubbery plateaus for zwitterionomers to similar strong ionic interactions between the zwitterionic functionalities.

Schmuck et al. demonstrated with a low molecular weight bis-zwitterion model that the zwitterionic species self-assembled in a head-to-tail fashion.[33] Bredas et al. predicted with theoretical calculations that the clustered zwitterions in polymers adopt an extended conformation with their dipoles aligning in an antiparallel

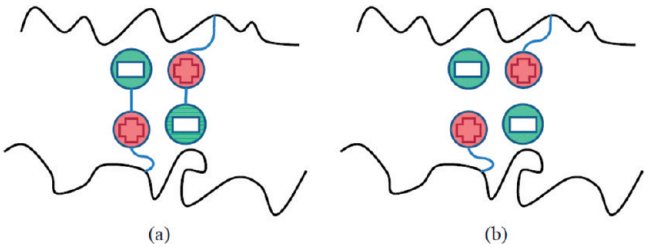

Figure 7. Simplified illustration of the possible charge interactions in (a) zwitterionomers and (b) cationic analogues.

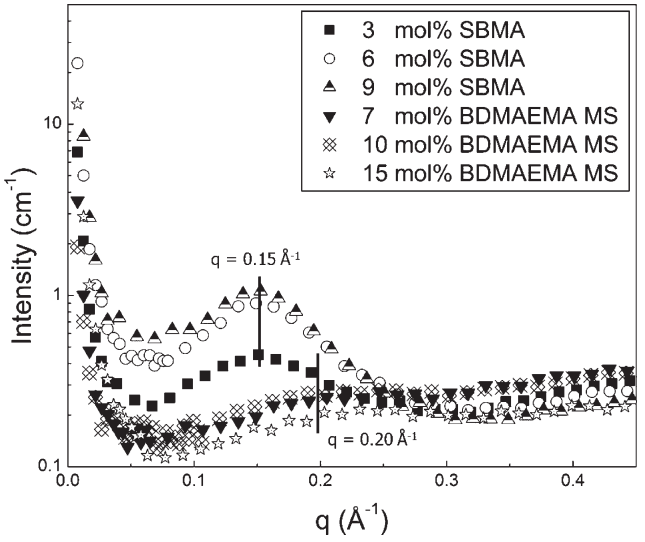

Figure 8. SAXS intensity vs scattering vector (q) traces for poly(nBA-*co*-SBMA) and poly(nBA-*co*-BDMAEMA MS) containing varying amounts of charged units.

fashion to favor interchain electrostatic interactions.[34] On the basis of these conclusions, we hypothesize that the charged zwitterions arrange in a head-to-tail fashion as illustrated in Figure 7a. Because of the covalent linkage between the cation and the anion on a zwitterion, the binding interactions between two zwitterionic functionalities represent ion−ion interactions (~250 kJ/mol).[35] In comparison, much weaker dipole−dipole interactions (~2 kJ/mol) between opposite charges are present in typical ionomers. The bulkiness of the quaternary ammonium cations in BDMAEMA MS, as well as their organic nature, should further contribute to the lack of rubbery plateau behavior for the cationic polymers. This is in agreement with what Page et al. reported for Nafion neutralized with alkylammonium cations;[36] however, experimental confirmation of such molecular level arrangements is lacking.

Morphologies of Zwitterionomers and Their Cationic Analogues. The morphologies of poly(nBA-*co*-SBMA) and poly(nBA-*co*-BDMAEMA MS) were probed using small-angle X-ray scattering (SAXS) and atomic force microscopy (AFM). Scattering profiles of the zwitterionomers and their cationic analogues, plotted as intensity vs the scattering vector magnitude, q, are shown in Figure 8. A scattering peak near $q \approx 0.15$ Å^{-1} was observed for each of the zwitterionomer samples, and the peak intensities decreased with decreasing sulfobetaine content in the copolymers. Scattering profiles containing such "ionomer peaks"

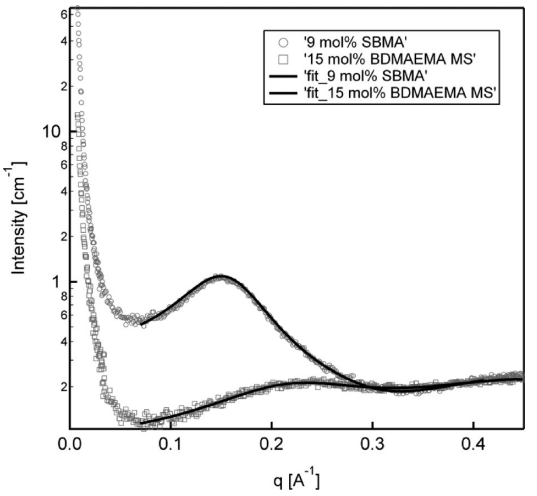

Figure 9. Fitting of representative SAXS traces of both the zwitterionomers and the cationic analogues to the Kinning−Thomas model.

are characteristic of charge-containing polymers.[15] The presence of the ionomer peaks was attributed to the different electron densities of the ionic aggregates and the surrounding matrix. These data indicated the presence of a microphase-separated morphology of zwitterion-rich domains in a matrix of nBA, consistent with the presence of physical cross-links as indicated using DMA. In comparison, the scattering peaks of the cationic analogues were very broad and weak with maxima around $q \approx 0.20$ Å^{-1}. The weaker scattering intensities for the cationic analogue samples suggested more phase mixing than the zwitterionomers in agreement with DSC findings.

The SAXS profiles of both the zwitterionomers and the cationic analogues were fit using a liquidlike interparticle interference model as proposed by Yarusso and Cooper and incorporating the Percus−Yevick structure factor, first used by Kinning and Thomas to model the scattering from spherical morphologies in block copolymers and later applied to ion-containing polymer by Ding et al.[37−40] The following general equation describes the scattered intensity of a sample from this model:

$$\frac{I}{I_e V} = \frac{1}{\nu_p}\left(\frac{4\pi {R_1}^3}{3}\right)^2 \Delta\rho^2 \Phi^2(qR_1) S(q, R_{ca}, R_1, \nu_p)$$

where I_e is the scattering from a single electron, V is the scattering volume, ν_p is the volume of material per ionic aggregate, R_1 is the radius of the ionic aggregate, R_{ca} is the radius of closest approach, and $\Delta\rho$ is the difference in electron densities between the ionic aggregates and the matrix. $\Phi(qR_1)$ and $S(q,R_{ca},R_1,\nu_p)$ are the form factor and the structure factor, respectively. The calculation of the Percus−Yevick structure factor followed the detailed expressions of Ding et al.[40] A Lorentzian peak, centered between 0.48 and 0.49 Å^{-1}, was added to the intensity function to represent poly(n-butyl acrylate) interchain scattering[41] and to improve the high-q fit. Figure 9 shows that the model fits the SAXS data of the 9 mol % SBMA sample and the 15 mol % BDMAEMA MS sample very well over the q range between 0.07 and 0.41 Å^{-1}. Similarly good fits were also obtained for the other samples investigated in this study. The fitting parameters ($\Delta\rho$, R_1, R_{ca}, and ν_p) as a function of copolymer contents are summarized in Table 3.

Table 3. Summary of the Fitting Parameters for Zwitterionomers and Their Cationic Analogues

copolymer composition	$\Delta\rho$ (10^{21} cm^{-3})	R_1 (nm)	R_{ca} (nm)	ν_p (nm^3)
poly(nBA$_{91}$-*co*-SBMA$_9$)	46.5	1.33	1.96	115
poly(nBA$_{94}$-*co*-SBMA$_6$)	46.6	1.27	1.96	112
poly(nBA$_{97}$-*co*-SBMA$_3$)	46.5	1.10	1.86	127
poly[nBA$_{85}$-*co*-(BDMAEMA MS)$_{15}$]	100	0.585	1.27	48.8
poly[nBA$_{90}$-*co*-(BDMAEMA MS)$_{10}$]	111	0.633	1.23	62.0
poly[nBA$_{93}$-*co*-(BDMAEMA MS)$_7$]	97.7	0.647	1.25	98.7

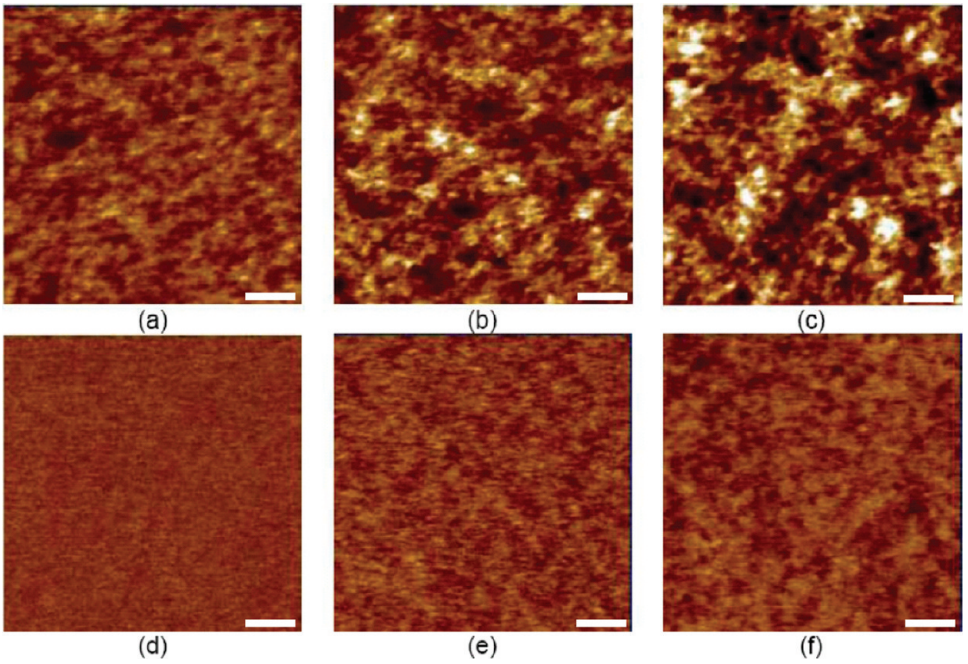

Figure 10. AFM phase images of zwitterionomers and their cationic analogues: samples a−c contain 3, 6, and 9 mol % SBMA, respectively; samples d−f contain 10, 15, and 22 mol % BDMAEMA MS, respectively. The scale bars are 100 nm; light phases represent higher modulus ionic aggregates.

The R_1 values for the zwitterionomers were close to what Ehrmann et al. reported for the R_g, which is a measure of the size of the scattering entities of similar zwitterionomers based on Guinier analysis.[14] The modeling of the SAXS data for quaternary ammonium-based cationomers is not well-documented in the literature. Hence, we compared our fits for the cationic analogues with those for common anionic ionomers and found that our R_1 values matched what Kutsumizu et al. and Tsujita et al. reported for partially neutralized poly(ethylene-*co*-methacrylic acid) ionomers.[42,43]

Increasing charge content appeared to lead to substantially different morphological changes between the zwitterionomers and their cationic analogues, although the weak scattering of the cationic analogues prevented drawing firm conclusions from the resulting fit parameters. Hence, the main focus of our data interpretation was on the trends in zwitterionomers. Specifically, an increase in charge content for the zwitterionomers resulted in an increase in R_1, the radius of the ionic aggregate, but very little change in ν_p. Since the density of ionic aggregates is proportional to $1/\nu_p$, these results suggested that the number of ionic aggregates per unit volume remained relatively constant with increasing charge content in the zwitterionomer series. Conversely, increasing charge content in the cationic analogues resulted in an increased number of smaller aggregates (decreasing R_1 and decreasing ν_p), as one can reliably conclude based on the weakly microphase-separated morphologies indicated by the scattering from the cationic analogues. However, this analysis of the SAXS data was in agreement with the DMA results for the zwitterionomers, as higher ion dissociation temperatures in DMA were observed for samples with higher charge contents, which also possessed larger ionic aggregates. Similar conclusions were not made for the cationic analogues as a rubbery plateau was not observed for any of the cationic analogues.

Furthermore, the comparison between the zwitterionomers and the cationic analogues revealed that the zwitterionomers contained fewer, but larger, ionic aggregates than the cationic analogues in a given sample volume. Considering that the rubbery plateaus in DMA were only observed for the zwitterionomers, the SAXS results supported our hypothesis that the binding interactions between the charges in the zwitterionomers were stronger than those in the cationic analogues.

AFM results are shown in Figure 10. For the zwitterionomers, clear evidence of surface microphase separation was observed at very low zwitterion incorporation of 3 mol %. In comparison, the surface of the cationic analogue that contained 10 mol % BDMAEMA MS appeared very smooth; even at 22 mol % of

charge composition, the cationic analogue still appeared less phase-separated than the 3 mol % zwitterionomer. This trend agreed with the SAXS findings. Because of different resolution limits of the two characterization techniques, the dimensions of the features observed using AFM are not comparable with those determined with SAXS. Nevertheless, the AFM results confirmed that the cationic analogues were more phase mixed than the zwitterionomers, consistent with the SAXS and DSC findings.

CONCLUSIONS

We successfully designed and synthesized BDMAEMA MS as the cationic analogue to SBMA. *n*BA-based acrylic copolymers containing SBMA and BDMAEMA MS of varying charge compositions were polymerized. ^{1}H NMR results showed good agreement between the monomer feed and copolymer compositions. The molecular weights of the copolymers were characterized using SEC in DMF with 0.01 M LiBr relative to polystyrene standards. Small- angle X-ray scattering traces from both zwitterionomers and cationic analogues were fit very well, using a hard-sphere model combined with a structure factor incorporating liquidlike interparticle interference.[37−40] The modeling results revealed that the zwitterionomers contained fewer, but larger, ionic aggregates than the cationic analogues in a given sample volume. The superior elastomeric performances observed for the zwitterionomers compared to their cationic analogues coincided with their more well-defined microphase-separated morphologies. The stronger ion−ion interactions in the zwitterionomers were thus postulated to produce rubbery plateaus in DMA and better mechanical performance. The stronger zwitterionic interaction offers the potential to uptake conductive diluents, such as ionic liquids, while maintaining their mechanical strength for advanced electromechanical applications. Future efforts may involve comparing the zwitterionomers with polymer blends and other more polar ionomers to further elucidate the impact of zwitterionic interactions.

ASSOCIATED CONTENT

Supporting Information. Detailed NMR and elemental analysis of BDMAEMA MS; composition analysis of poly(*n*BA-*co*-SBMA) and poly(*n*BA-*co*-BDMAEMA MS) using ^{1}H NMR spectroscopy. This material is available free of charge via the Internet at http://pubs.acs.org.

AUTHOR INFORMATION

Corresponding Author

*E-mail: rick.beyer@us.army.mil (F.L.B.); telong@vt.edu (T.E.L.).

ACKNOWLEDGMENT

This material is based upon work supported by the U.S. Army Research Laboratory and the U.S. Army Research Office under Grant W911NF-07-1-0339. Parts of this work were carried out using instruments in the Nanoscale Characterization and Fabrication Laboratory, a Virginia Tech facility operated by the Institute for Critical Technology and Applied Science. The authors also acknowledge Dr. Andrew Duncan at the U.S. Army Research Laboratory for his assistance with the collection of small-angle X-ray scattering data.

REFERENCES

(1) Mauritz, K. A.; Moore, R. B. *Chem. Rev.* **2004**, *104* (10), 4535.
(2) Duncan, A. J.; Leo, D. J.; Long, T. E. *Macromolecules* **2008**, *41* (21), 7765.
(3) Williams, S. R.; Long, T. E. *Prog. Polym. Sci.* **2009**, *34* (8), 762.
(4) Hickner, M. A.; Ghassemi, H.; Kim, Y. S.; Einsla, B. R.; McGrath, J. E. *Chem. Rev.* **2004**, *104* (10), 4587.
(5) Park, H. B.; Freeman, B. D.; Zhang, Z.-B.; Sankir, M.; McGrath, J. E. *Angew. Chem., Int. Ed.* **2008**, *47* (32), 6019.
(6) De Smedt, S. C.; Demeester, J.; Hennink, W. E. *Pharm. Res.* **2000**, *17* (2), 113.
(7) Duncan, A. J.; Leo, D. J.; Long, T. E.; Akle, B. J.; Park, J. K.; Moore, R. B. *Proc. SPIE* **2009**, 728711/1–728711/11.
(8) Brown, R. H.; Duncan, A. J.; Choi, J. H.; Park, J. K.; Wu, T. Y.; Leo, D. J.; Winey, K. I.; Moore, R. B.; Long, T. E. *Macromolecules* **2010**, *43* (2), 790.
(9) Galin, M.; Chapoton, A.; Galin, J. C. *J. Chem. Soc., Perkin Trans.* **1993**, *2*, 545.
(10) Ehrmann, M.; Muller, R.; Galin, J. C.; Bazuin, C. G. *Macromolecules* **1993**, *26* (18), 4910.
(11) Mathis, A.; Zheng, Y. L.; Galin, J. C. *Polymer* **1991**, *32* (17), 3080.
(12) Ehrmann, M.; Galin, J. C. *Polymer* **1992**, *33* (4), 859.
(13) Ehrmann, M.; Galin, J. C.; Meurer, B. *Macromolecules* **1993**, *26* (5), 988.
(14) Ehrmann, M.; Mathis, A.; Meurer, B.; Scheer, M.; Galin, J. C. *Macromolecules* **1992**, *25* (8), 2261.
(15) Eisenberg, A.; Hird, B.; Moore, R. B. *Macromolecules* **1990**, *23* (18), 4098.
(16) Koberle, P.; Laschewsky, A. *Macromolecules* **1994**, *27* (8), 2165.
(17) Galin, M.; Marchal, E.; Mathis, A.; Galin, J. C. *Polym. Adv. Technol.* **1997**, *8*, 75.
(18) Galin, M.; Marchal, E.; Mathis, A.; Meurer, B.; Soto, Y. M. M.; Galin, J. C. *Polymer* **1987**, *28* (11), 1937.
(19) Lee, W.-F.; Lee, C.-H. *Polymer* **1997**, *38* (4), 971.
(20) Lee, W.-F.; Tsai, C.-C. *Polymer* **1994**, *35* (10), 2210.
(21) Lee, W.-F.; Tsai, C.-C. *Polymer* **1995**, *36* (2), 357.
(22) Ilavsky, J.; Jemian, P. R. *J. Appl. Crystallogr.* **2009**, *42* (2), 347.
(23) Hamid, S. M.; Sherrington, D. C. *Polymer* **1987**, *28* (2), 325.
(24) Oya, T.; Kunita, K.; Araki, K.; Iwai, Y.; Sonokawa, K.; Sasaki, T. Lithographic printing plate precursor and lithographic printing method. EP 2006738 A2 2008-11283, Application: EP, 2008.
(25) Ushakova, V. N.; Kipper, A. I.; Afanakina, N. A.; Samarova, O. E.; Klenin, S. I.; Panarin, E. F. *Vysokomol. Soedin., Ser. A, Ser. B* **1995**, *37* (6), 933.
(26) Yuan, H.; Li, C.; Zhu, Y.; Huang, B. Manufacture of amphiphilic cation flocculant with high molecular weight for wastewater treatment. CN 1721339 A 20060118, Application: CN, 2006.
(27) Layman, J. M.; Borgerding, E. M.; Williams, S. R.; Heath, W. H.; Long, T. E. *Macromolecules* **2008**, *41* (13), 4635.
(28) Tong, J. D.; Jerome, R. *Polymer* **2000**, *41* (7), 2499.
(29) Ahmad, N. M.; Charleux, B.; Farcet, C.; Ferguson, C. J.; Gaynor, S. G.; Hawkett, B. S.; Heatley, F.; Klumperman, B.; Konkolewicz, D.; Lovell, P. A.; Matyjaszewski, K.; Venkatesh, R. *Macromol. Rapid Commun.* **2009**, *30* (23), 2002.
(30) Barner-Kowollik, C. *Macromol. Rapid Commun.* **2009**, *30* (23), 1961.
(31) Burch, R. R.; Manring, L. E. *Macromolecules* **1991**, *24* (8), 1731.
(32) Gauthier, M.; Eisenberg, A. *Macromolecules* **1990**, *23* (7), 2066.
(33) Schmuck, C.; Rehm, T.; Klein, K.; Gröhn, F. *Angew. Chem., Int. Ed.* **2007**, *46* (10), 1693.
(34) Bredas, J. L.; Chance, R. R.; Silbey, R. *Macromolecules* **1988**, *21* (6), 1633.
(35) Atkins, P.; de Paula, J. In *Atkins' Physical Chemistry*, 7th ed.; Oxford University Press: New York, 2002; p 700.
(36) Page, K. A.; Cable, K. M.; Moore, R. B. *Macromolecules* **2005**, *38* (15), 6472.

(37) Yarusso, D. J.; Cooper, S. L. *Macromolecules* **1983**, *16* (12), 1871.
(38) Percus, J. K.; Yevick, G. J. *Phys. Rev.* **1958**, *110*, 1.
(39) Kinning, D. J.; Thomas, E. L. *Macromolecules* **1984**, *17* (9), 1712.
(40) Ding, Y. S.; Register, R. A.; Yang, C.; Cooper, S. L. *Polymer* **1989**, *30* (7), 1213.
(41) Miller, R. L.; Boyer, R. F.; Heijboer, J. *J. Polym. Sci., Polym. Phys. Ed.* **1984**, *22* (12), 2021.
(42) Kutsumizu, S.; Tagawa, H.; Muroga, Y.; Yano, S. *Macromolecules* **2000**, *33* (10), 3818.
(43) Tsujita, Y.; Hayashi, N.; Yamamoto, Y.; Yoshimizu, H.; Kinoshita, T.; Matsumoto, S. *J. Polym. Sci., Part B: Polym. Phys.* **2000**, *38* (10), 1307.